Wave Inversion Technology, Report No. 4, pages 263-274

Attenuation of Primary Multiples and Peg-legs: Comparison of WHL and KBC Methods.

Lourenildo W. B. Leite, Marcus P. C. da Rocha and Fábio J. Alves[1]

keywords: *Multiple suppression, Predictive deconvolution*

ABSTRACT

The KBC and WHL methods are here compared and applied to the multiple suppression of peg-legs related to upper low velocity layers (weathering zone) and to deeper high velocity layers (diabase sills).

INTRODUCTION

The general aim of the present report is to present some results of the comparison of the methods of Wiener-Hopf-Levenberg (WHL), and of Kalman-Bucy-Crump (KBC) to resolve the problem of reconstructing the medium reflectivity response by deconvolving the source-time effective function from observed data.

The specific aim of the present report is to resume the activities developed towards the study of multiple suppression related to an upper low velocity layer (weathering zone), and of the peg-leg related to the same low velocity layer and to a deeper high velocity layer (diabase sills), and also to establish new problems. This situation is considered as typically encountered in the Amazon sedimentary basin to where our attentions are aimed at. The amount of seismic data is rather large, and as they deserve more attention other processing and interpretation problems solutions are naturally submitted. The challenge is mathematically related to the general representation of inverse problems.

THE A PRIORI KNOWLEDGE

The components of the convolutional model are described in canonic form to be in accordance with an uniform discretization established in the Goupillaud solution of two-way unitary travel-time that uses the unilateral Laplace Z-transform (LZT).

[1]**email:** mrocha@ufpa.br

A discrete description of the 1D convolutional model for the representation of seismic data, $g(k)$, independent of the horizontal ray parameter p, is given by:

$$g(k) = m(k) + n(k) = s(k) * \epsilon(k) + n(k). \tag{1}$$

Where $s(k)$ represents the effective source-pulse, $\epsilon(k)$ is the reflectivity function, $m(k)$ is the signal-message, and $n(k)$ is the eternal temptative to be described as the additive signal-noise not accounted for in $\epsilon(n)$ and in $s(k)$.

The source time history is represented by the Berlage function:

$$f(t) = Au(t)t^n e^{-\gamma t} cos(2\pi f_0 t + \phi_0), \tag{2}$$

where $f_0 = 32,5$ Hz and $\phi_0 = 30$ rd.

We aim at to construct the seismic reflection trace by the convolutional model based on Betti's theorem. The physics of propagation is governed by the equation of particle motion in the 1-D acoustic form: $\rho(x)\partial_t^2 g(x,t) = \partial_x[E(x)\partial_x g(x,t)]$. The phenomenon is of an incident vertical plane wave on a medium formed by horizontal, homogeneous and isotropic layers. The boundary conditions of displacement (or pressure) and stress continuity result in defining the reflection, r_k, and the transmission, t_k, coefficients for the interface k between the layers k and $k+1$, that results in: $r_k = (I_k - I_{k+1})/(I_k + I_{k+1})$, $t_k = 2I_k/(I_k + I_{k+1})$, where r_k and t_k are real numbers, $t_k + r_k = 1, \quad \mid r_k \mid \leq 1$ and $0 \leq t_k \leq 2$. The physical problem now has been transformed to a physics of interfaces, and the events making the seismic trace are considered as primary and secondary reflections (multiples).

The relation between the descendent, $D(z)$, and the ascendent, $U(z)$, waves, and between the top, $k = 0$, and the bottom, $k = K+1$, is expressed by the matricial propagator:

$$\begin{bmatrix} D_{K+1}(z) \\ U_{K+1}(z) \end{bmatrix} = \frac{z^{-K/2}}{(1-r_K)(1-r_{k-1})...(1-r_2)(1-r_1)} N_K ... N_1 N_0 \begin{bmatrix} D_0(z) \\ U_0(z) \end{bmatrix}. \tag{3}$$

The reflection transfer function for a system of K layers is given by:

$$R(z) = R_K(z) = \frac{U_0(z)}{D_0(z)} = \frac{r_0 P_k(z) - Q_k(z)}{P_k(z) - r_0 Q_k(z)}. \tag{4}$$

The denominator $P_k(z) - r_0 Q_k(z)$ has the property of being of minimum-phase. The numerator $r_0 P_k(z) - Q_k(z)$ is not necessarily of minimum-phase, what makes $R(z)$ be or not to be of minimum-phase. The polynomial division is ilimited, but numerically made to correspond to the number of layers K.

In special conditions for analyses we can admit $\epsilon(n) \approx r(n)$, or yet that $\epsilon(n) = r(n)$. A total response $\epsilon(n)$ is composed of the primary incident field and of the secondary spread out field, and the figures show how the secondary field can gradually

have the same importance as that of the primary field has along the trace (see Figure 1 and 2).

The WHL filter governing equations is a natural stationary model, and the filter $h(t)$ is the unknown time-invariant operator that is constrained to satisfy a desired output $d(t)$ through the commonly referred to as the Wiener-Hopf integral equation. We continue with the equations in the convenient canonic forms, with a uniform discretization as already established in the Goupillaud model. The criteria for the filter is the minimization of the variance error, $e(k) = \hat{g}(k) - d(k)$, between $d(k)$ (desired signal) and $\hat{g}(k)$ (real output) in time domain:

$$I(h_i) = E\left\{\left[\sum_{k=1}^{N} \hat{g}(k) - d(k)\right]^2\right\}. \tag{5}$$

The filter real output is simply: $\hat{g}(k) = h(k) * g(k)$. The minimization of $I(h_i)$ results in the general WHL equation:

$$\sum_{k=1}^{N} h(k)\phi_{gg}(l-k) = \phi_{dg}(l). \tag{6}$$

The solution defines the coefficients $h(k)$ which depends on what kind of operation is to be intended for, and accomplished by a priori conditions. $\phi_{gg}(.)$ represents the theoretical autocorrelation of the input, and $\phi_{dg}(.)$ is the theoretical stochastic unilateral crosscorrelation between the desired and the observed signals. The filter quality is here also measured by the formula of the normalized minimum error given by the summation:

$$I_{min} = 1 - [\phi_{gg}(0)]^{-1} \sum_{k} \phi_{dg}(k)h(k). \tag{7}$$

The KBC filter governing equations in a natural non-stationary model, and the data window does not satisfy the principles underlined by the convolution integral. For this reason, the equation is rewritten in the form of a moving average according to the commonly referred to as the Wiener-Kolmolgorov problem, and it is expressed by the matrix integral equation:

$$\underline{\underline{\phi}}_{dg}(t,\sigma) = \int_{t_0}^{t} \underline{\underline{h}}_K(t,\tau)\underline{\underline{\phi}}_{gg}(\tau,\sigma)d\tau, \quad (t_0 \le \tau, \sigma \le t), \quad \underline{\hat{g}}(t) = \int_{t_0}^{t} \underline{\underline{h}}_K(t,\tau)\underline{g}(\tau)d\tau, \tag{8}$$

where $\underline{\hat{g}}(t)$ is the actual output, and $\underline{\underline{h}}_K(t,\tau)$ is the corresponding desired optimum time-variant operator. The criterion used is the minimization of the residue covariance expressed as:

$$I(h) = E\left[\left\{\underline{\hat{g}}(t) - \underline{d}(t)\right\}^2\right]. \tag{9}$$

The formulation has for basis expressing the response of any system by an ordinary differential equation of order $N-1$

$$\sum_{n=0}^{N-1} a_n(t)\frac{d^n y(t)}{dt^n} = w(t), \qquad (a_1 = 1). \tag{10}$$

The transformation to the state variable $x_n(t)$ and $\dot{x}_n(t)$ is by substituting the higher derivatives of $y(t)$. The resulting dynamic state equation in the general (continuous, time-variant) compact form are:

$$\dot{\underline{x}}(t) = \underline{\underline{F}}(t)\underline{x}(t) + \underline{\underline{G}}(t)\underline{w}(t), \quad \text{(system)}, \tag{11}$$

$$\underline{z}(t) = \underline{y}(t) + \underline{v}(t) = \underline{\underline{H}}(t)\underline{x}(t) + \underline{v}(t), \quad \text{(output)}. \tag{12}$$

$\underline{\underline{F}}(t)$, $\underline{\underline{G}}(t)$ and $\underline{\underline{H}}(t)$ are matrices with variable elements in t; $\underline{w}(t)$ is the forcing function that generates the state; $\underline{z}(t)$ is the selected form for the output given by the structure of the matrix $\underline{\underline{H}}(t)$; $\underline{v}(t)$ is the addtive noise present.

The continuous form solution is given by the system of three coupled equations:

(1) $\frac{d\hat{\underline{x}}(t)}{dt} = \left[\underline{\underline{F}}(t) - \underline{\underline{K}}(t)\underline{\underline{H}}(t)\right]\hat{\underline{x}}(t) + \underline{\underline{K}}(t)\underline{z}(t)$, (state estimation differential equation)

(2) $\underline{\underline{K}}(t) = \underline{\underline{P}}(t)\underline{\underline{H}}^T(t)\underline{\underline{V}}^{-1}(t)$, (the gain matrix);

(3) $\dot{\underline{\underline{P}}}(t) = \underline{\underline{F}}(t)\underline{\underline{P}}(t) + \underline{\underline{P}}(t)\underline{\underline{F}}^T(t) - \underline{\underline{P}}(t)\underline{\underline{H}}^T(t)\underline{\underline{V}}^{-1}(t)\underline{\underline{H}}^T(t)\underline{\underline{P}}(t) + \underline{\underline{G}}(t)\underline{\underline{Q}}(t)\underline{\underline{G}}^T(t)$, (the Ricatti non-linear differential equation).

DEVELOPMENT OF THE ALGORITHMS WHL AND KBC

The WHL solution in discrete form to the problem under analysis is a modified classical prediction operator for multiple attenuation. We resume as:

(a) The desired output: $d(k) = m(k+T)$, where T is the prediction distance;

(b) The WHL equation in parametric form: $\sum_k h(k)\left[\phi_{ss}(k) + \sigma_n^2\delta(k)\right] = \phi_{ss}(l+T)$.

(c) The WHL prediction operator with a rectangular window $C(l)$ to select out the events to be suppressed is represented by the equation $\sum_{k=1}^{N} h(k)\phi_{gg}(l-k) = C(i-i_0)\phi_{gg}(l+T)$.

An example intentionally simple is the case of multiples not accounted for in $\epsilon(k)$, represented as a delayed pulse of T units (T= layer thickness/layer velocity) with a generalization through the following function: $f(k) = \sum_{i=0}^{I} r_i s(k-T_i)$, which results in an autocorrelation of the form: $\phi_{gg}(k) \approx \phi_{ff}(k) = \sum_{i=0}^{I}\sum_{l=0}^{I} r_i r_l \phi_{ss}(k - T_i + T_l)$.

The first term of the series is $\sigma_r^2 \phi_{ss}(k)$, where the variance $\sigma_r^2 = \sum_{i=0}^{I} r_i^2$ modifies the desired segment $\phi_{ss}(k)$, and the deconvolutional operator has a factor that scales the desired $\epsilon(k)$. From this we conclude that for windowing $\phi_{ss}(k)$ it is necessary that the lengths of the source-pulse and of the temporal window for truncation and smoothing do not contain the first multiple at distance T_1. Consequently, the elongated operator with T_1 deconvolves the multiple of period T_1, and the operator with length $T_1 + T_2$ deconvolves the multiples T_1 and T_2, and so on. (see Figure 2 and 3)

The application of the KBC solution in discrete form to a seismic trace, $z(k)$, consists in a sequence of point-to-point operations organized in a definite sequence. The matrix $P(k)$ computed as:

$$\underline{\underline{P}}^{+}(k) = \underline{\underline{\Phi}}(k, k-1)\underline{\underline{P}}^{-}(k-1)\underline{\underline{\Phi}}^{T}(k, k-1) + \underline{\underline{Q}}(k-1), \tag{13}$$

$$\underline{\underline{P}}^{-}(k) = \underline{\underline{P}}^{+}(k) - \underline{\underline{K}}(k)\underline{\underline{H}}(k)\underline{\underline{P}}^{+}(k), \tag{14}$$

where $\Phi(k, k-1)$ is the state transition matrix. The gain matrix $K(k)$ is calculated by:

$$\underline{\underline{K}}(k) = \underline{\underline{P}}^{+}(k)\underline{\underline{H}}^{T}(k)\left\{\underline{\underline{H}}(k)\underline{\underline{P}}^{+}(k)\underline{\underline{H}}^{T}(k) + \underline{\underline{R}}(k)\right\}^{-1}. \tag{15}$$

The state vector is calculated by:

$$\underline{\hat{x}}^{+}(k) = \underline{\hat{x}}^{-}(k) + \underline{\underline{K}}(k)\left[\underline{z}(k) - \underline{\hat{x}}^{-}(k)\right]; \quad \underline{\hat{x}}^{+}(k) = \underline{\underline{\Phi}}(k, k-1)\underline{\hat{x}}^{-}(k-1); \tag{16}$$

And the output has the expression: $\underline{z}^{+}(k) = \underline{\underline{H}}(k)\underline{x}^{+}(k)$. The strategy is to recover the multiple-free sismogram.

We start identifying the variable with the non-stationary model. The seismic pulse is represented by the matrix: $H_{ji} = s_j(i)$. The selection of the state vector is nonunique, and in this case the is defined as:

$$\underline{x}(k) = [g(k) \quad g(k-1) \quad ... \quad g(k-L+1)]. \tag{17}$$

The dynamic equations of the system to establish the recursive process of generation of the state vector is completed by the following model:

$$g(k) = \sum_{i=1}^{L} b_i(k-1)g(k-1) + v_2(k-1), \tag{18}$$

$v_2(k)$ is theoretically considered as a white stochastic process. This equation projects the trace forward through a weighed sum of L previous values in a similar formalism to the WHL. The coefficients $b_i(k)$ are defined by a chosen model and experimentation, and in the present case has been the exponential model. The state is written as

$$\underline{x}(k) = \underline{\underline{\Phi}}(k, k-1)\underline{x}(k-1) + \underline{g}\underline{v}_2(k-1). \tag{19}$$

NUMERICAL RESULTS

We constructed two basic models for showing and comparing the WHL and KBC operators in multiple attenuation, where undesirable effects from sills and from low velocity upper layers are suppressed, and information from lower target layers (low acoustic impedance) are better stressed. The first model is formed by 4 layers over a half-space (Figure1), and the second model is formed by 250 layers over a half-space (Figure 4). The layer thickness vary from 1 to 20 meters. This second model tries to simulate the estratigraphy of the Amazon sedimentary basin.

Figures 2 and 3 show the results of the WHL and KBC operators for the simple model (4 layers) described in Figure 1. In Figure 2 we observe the good performance of both operators (WHL and KBC) in suppressing the peg-leg, and also that the WHL shows to be a somewhat better than the KBC. In Figure 3 we interpret by marking the different events on the seismic trace and on its autocorrelation. It is also marked the window $C(k)$ that selects out the event to be treated.

Figures 5 to 8 show the results of the WHL and KBC operators for the complex model (250 layers) described in Figure 4. Figure 5 we interpret by marking the different events on the sismic trace and on its autocorrelation. It is also marked the window that selects the events to be treated. In Figure 6 we observe the good performance of both operators (WHL and KBC) in suppressing several peg-legs, and also that the WHL shows to be somewhat better than the KBC. The final shown results of the WHL and KBC were obtained only after two consecutive deconvolutions, where the first output serves as input for the second deconvolution. The results of each WHL deconvolution, and the marking of the windows on the autocorrelation for selecting the events to be treated are shown in Figures 7 and 8, respectively.

CONCLUSIONS

One advantage for implementing the WHL with respect to the KBC was the facility for selecting the event to be treated, besides the possibility to include more than one event in one suppression process. The KBC operator performs this same operation by making use of a direct model obtained from a well-log. The attenuation of the multiples (after primaries and peg-leg) produced by our model of diabase sills clearly shows that the of presence lower layers become more evident. The form of the trace of the WHL operator becomes more complex as the quantity of selected events are include in the truncating window. On the other hand, the KBC operation takes care of one event at a time. The comparison of the WHL and KBC techniques show that the a implementation of the KBC can be simpler than the WHL, on the other hand, the experiments show that the WHL is a little more efficient in resolution than the KBC.

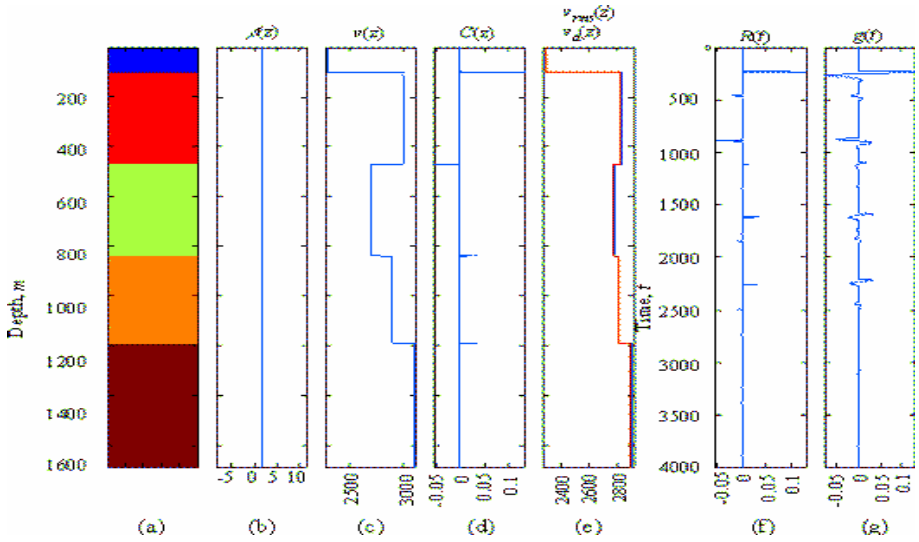

Figure 1: Simple model for operator analyses. (a) Geological section. (b) Density log. (c) Velocity log. (d) Distribution of reflection coefficients. (e) RMS log and Average velocities. (f) Reflectivity. (g) Seismic trace obtained by convolution between the medium impulse response calculated by the Goupillaud (f) solution with an effective source pulse (Berlage function).

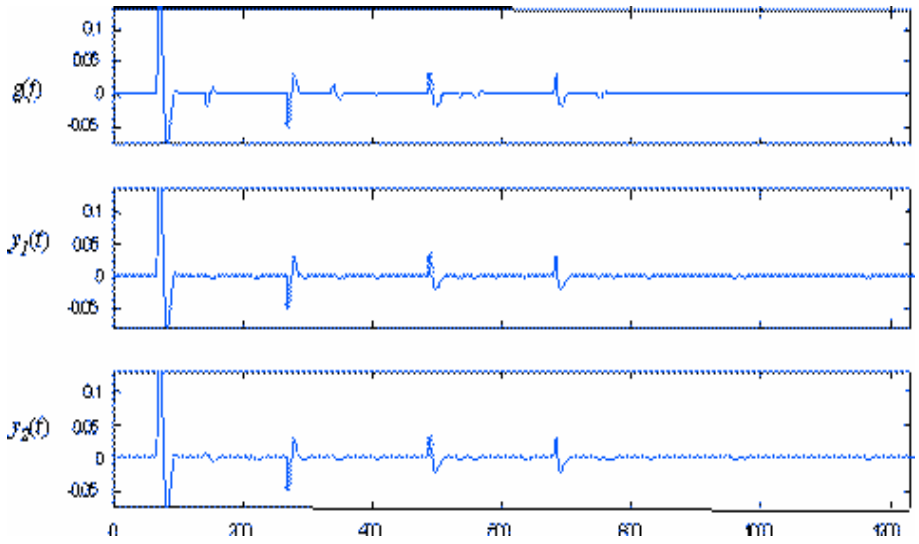

Figure 2: Simple model for operator analyses. $g(t)$ is the seismic trace. $y_1(t)$ is the WHL filter output. $y_2(t)$ is the KBC filter output. As a comparison, the multiple suppression by WHL looks better than the KBC output.

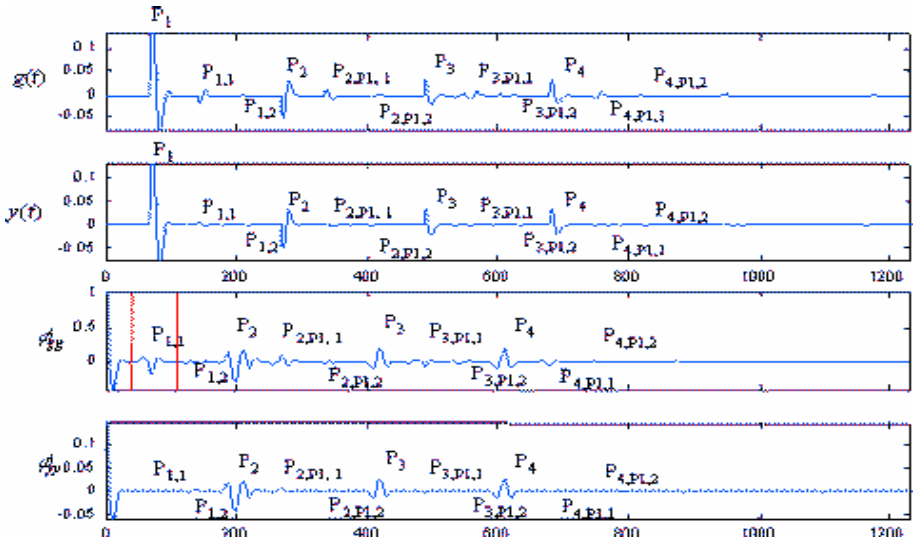

Figure 3: Simple model for operator analyses. We stress on the interpretation of the autocorrelation. $g(t)$ is the seismic trace. $y(t)$ is the filter output. ϕ_{gg} is the input autocorrelation. ϕ_{yy} is autocorrelation of the output. P_1, P_2, P_3 and P_4 represent the primary reflections from the first, second, third and forth interface, respectively. $P_{1,1}$ and $P_{1,2}$ are the multiples from the first interface. $P_{2,P1,1}$, $P_{2,P1,2}$, $P_{3,P1,1}$, $P_{3,P1,2}$, $P_{4,P1,1}$ and $P_{4,P1,2}$, are the peg-legs from the second, third and fourth interfaces.

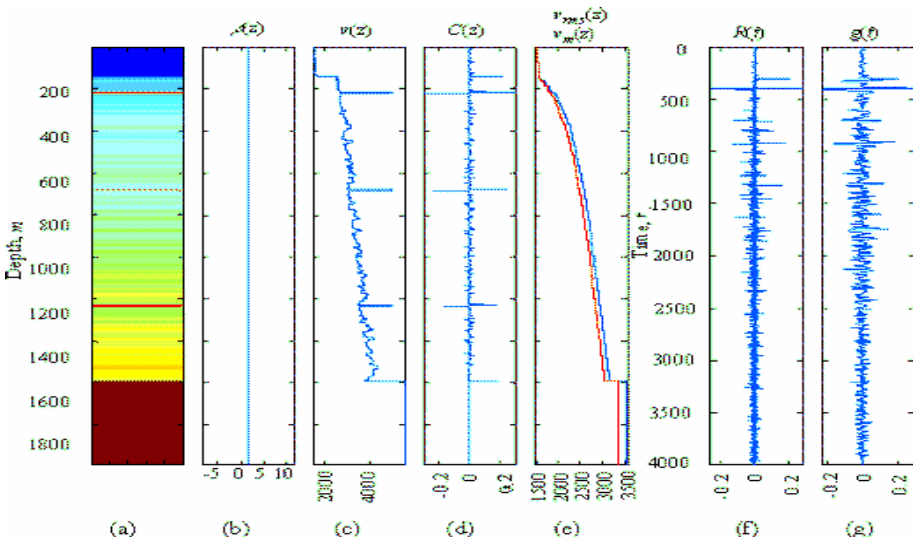

Figure 4: Complex model for operator analyses. (a) Geological section. (b) Density log. (c) Velocity log. (d) Distribution of reflection coefficients. (e) RMS log and Average velocities. (f) Reflectivity. (g) Seismic trace obtained by convolution between the medium impulse response calculated by the Goupillaud solution (f) with an effective source pulse (Berlage function).

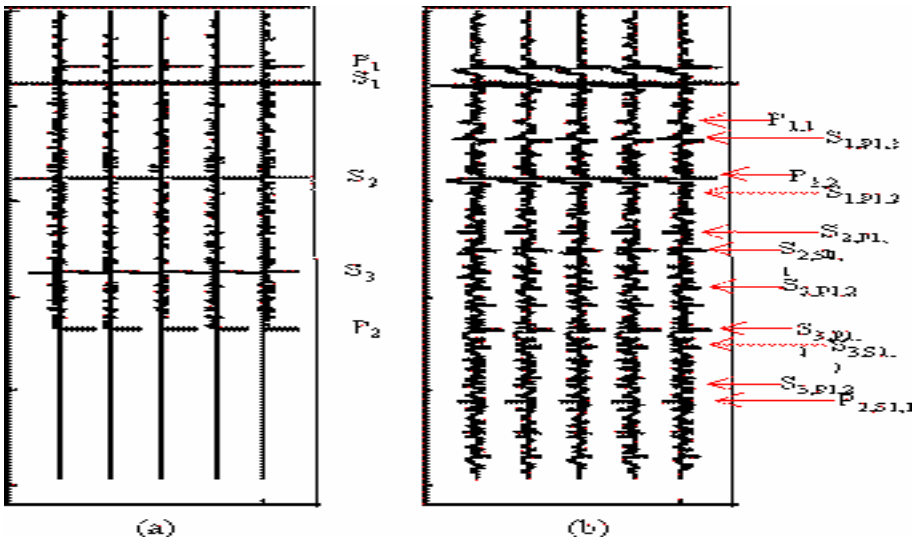

Figure 5: (a) Distribution of reflection coefficients. (b) Seismogram. P_1 represents the reflections from an interface that separates the upper low velocity layers from the lower high velocity layers. S_1, S_2 and S_3 are the sequential reflections from sills layers. P_2 represent the reflection from the basement interface. $P_{1,1}$ and $P_{1,2}$ represent the first and the second multiple from P_1. $S_{1,P1,1}$ and $S_{1,P1,2}$ are the peg-legs from the top of the first sill layer on the interface that corresponds to P_1. $S_{2,P1,1}$ and $S_{2,P1,2}$ are the peg-legs from the second sill on the interface that corresponds to P_1. $S_{3,P1,1}$ and $S_{3,P1,2}$ are the peg-legs from the third sill on the interface that corresponds to P_1. $S_{2,S1,1}$ and $S_{3,S1,2}$ are the peg-legs from the second and third sill layer on the interface from the first sill. $P_{2,S1,1}$ is the peg-leg from the reflection of the basement to the first sill.

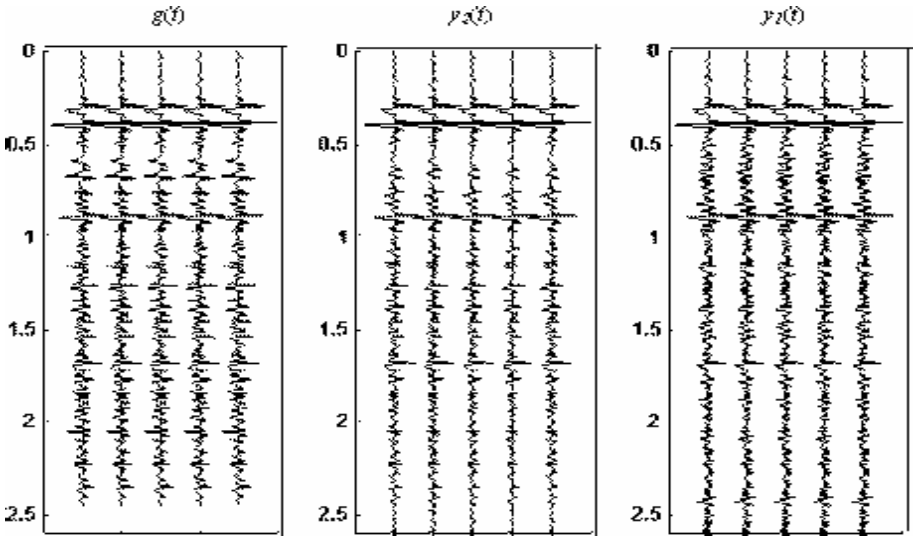

Figure 6: Complex model for operator analyses. $g(t)$ is the seismic trace. $y_1(t)$ is the WHL filter output. $y_2(t)$ is the KBC filter output. As a comparison, the multiple suppression by WHL gives a better result than the KBC output. The primary information from the deeper layers is better recognized.

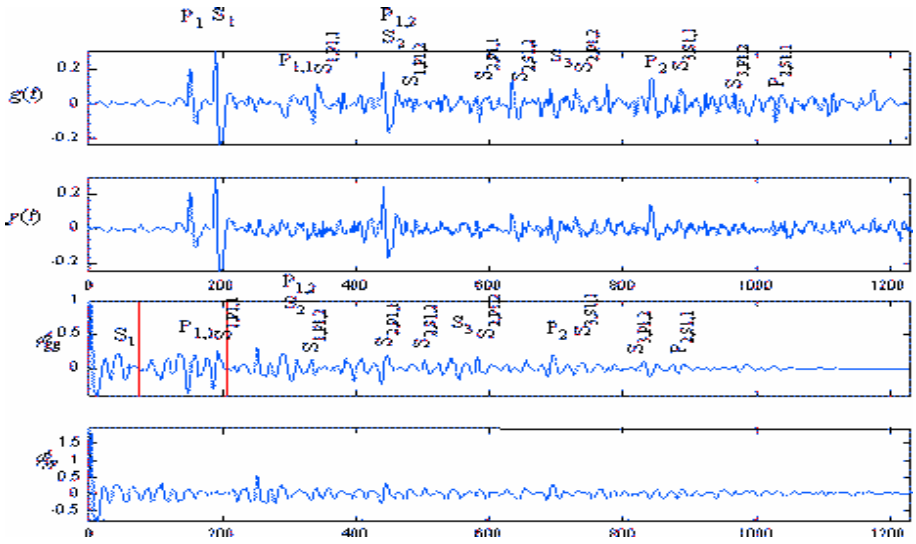

Figure 7: $g(t)$ is the seismic trace. $y(t)$is the deconvolved trace. ϕ_{gg} is the autocorrelation of the input. ϕ_{yy} is the autocorrelation of the output. The vertical lines on ϕ_{gg} represent the limits of the rectangular window for selecting the events to be suppressed. We observe in the deconvolved trace, and in its autocorrelation, that the events $P_{1,1}$ and $S_{1,P1}$ are attenuated.

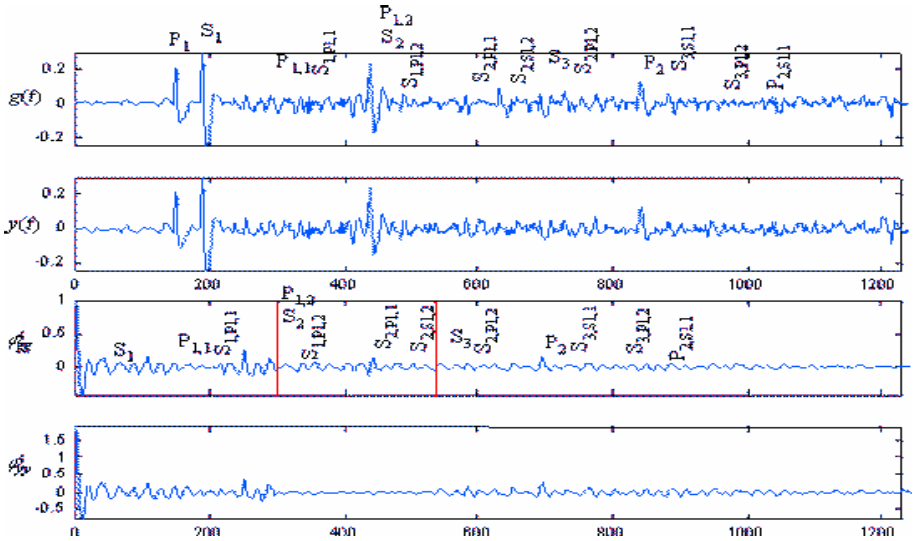

Figure 8: $g(t)$ is the output of the previous deconvolution on the seismic trace of Figure 7. $y(t)$ is the twofold deconvolved trace. ϕ_{gg} is the input autocorrelation. ϕ_{yy} is the autocorrelation of the output. The vertical lines on ϕ_{gg} represent the limits of the rectangular window used. We observe in the deconvolved trace, and in its autocorrelation, that the events are attenuatted, besides the second deconvolution incresed the resolution measured qualitatively.

REFERENCES

Aldridge, D. F. (1990). The Berlage Wavelet. Geophysics, 55(1):1508-1511.

Bayless, J.W. and Brigham, E. (1970). Application of the Kalman filter to continuous signal restoration. Geophysics, v. 35, n. 1, p. 2-23.

Burridge, G.S. Papanicolaou and B.S. White (1988). One-dimensional wave propagation in a highly discontinuous medium. Wave Motion, v. 10, p. 19-44.

Crump, N. (1974). A Kalman filter approach to the deconvolution of seismic signals. Geophysics, v. 39, n. 1, p. 1-13.

Kalman, R.E. and Bucy, R.E. (1961). New results in linear filtering and prediction theory. ASME, Series D, Journal of Basic Engineering, 82, 35-45.

Khattri, K. and Gir, R. (1976). A study of the seismic signatures of sedimentary models using synthetic seismograms. Geophysical Prospecting, v. 24, n. 3, p. 454-477.

Mendel, J.M. (1983). Optimal Seismic Deconvolution. An Estimation-Based Approach. Academic press. New York, USA.

Rocha, M.P.C. (1998). Application of the Kalman Method to Geophysical Data. Masters thesis. Graduate Course in Geophysics, Federal University of Pará. Brazil. (in Portuguese).